

Highlights

MC-ViT: Multi-branch Classifier-ViT to Detect Mild Cognitive Impairment in Older Adults Using Facial Videos

Jian Sun, Hiroko Hayama Dodge, Mohammad H. Mahoor

- We propose MC-ViT to detect MCI from the interview videos provided by the I-CONECT Study.
- We design the MC module to enrich the extracted spatio-temporal features. Its multi-branch structure helps ViViT to capture the visual features from different perspectives.
- We develop the HP loss by combining Focal loss and AD-CORRE loss. The HP loss addresses the inter- and intra-class imbalanced issues and helps the model pay attention to classes with less samples and subjects with short video length.
- We predict MCI from NC by analyzing the semi-structured interview videos.

MC-ViT: Multi-branch Classifier-ViT to Detect Mild Cognitive Impairment in Older Adults Using Facial Videos

Jian Sun^{a,1}, Hiroko Hayama Dodge^{b,2} and Mohammad H. Mahoor^{c,*,3}

^aDepartment Of Computer Science, University of Denver, 2155 E Wesley Ave, Denver, Colorado, 80210, United States of America

^bDepartment Of Neurology at Harvard Medical School, Harvard University, Massachusetts General Hospital, 55 Fruit St, Boston, Massachusetts, 02114, United States of America

^cDepartment Of Computer Engineering, University of Denver, 2155 E Wesley Ave, Denver, Colorado, 80210, United States of America

ARTICLE INFO

Keywords:

Deep Learning,
Facial Expression Features,
Inter- and Intra-class imbalance,
Mild Cognitive Impairment,
Multi-branch Classifier,
Transformer, ViT.

ABSTRACT

Deep machine learning models including Convolutional Neural Networks (CNN) have been successful in the detection of Mild Cognitive Impairment (MCI) using medical images, questionnaires, and videos. This paper proposes a novel Multi-branch Classifier-Video Vision Transformer (MC-ViT) model to distinguish MCI from those with normal cognition by analyzing facial features. The data comes from the I-CONECT, a behavioral intervention trial aimed at improving cognitive function by providing frequent video chats. MC-ViT extracts spatiotemporal features of videos in one branch and augments representations by the MC module. The I-CONECT dataset is challenging as the dataset is imbalanced containing Hard-Easy and Positive-Negative samples, which impedes the performance of MC-ViT. We propose a loss function for Hard-Easy and Positive-Negative Samples (HP Loss) by combining Focal loss and AD-CORRE loss to address the imbalanced problem. Our experimental results on the I-CONECT dataset show the great potential of MC-ViT in predicting MCI with a high accuracy of 90.63% accuracy on some of the interview videos.

1. Introduction

Alzheimer's disease (AD) and related dementias (ADRD) are national public health issues with pervasive challenges for older adults, their families, and caregivers. ADRD is not only ranked as the sixth-leading cause of death in the U.S., but the COVID-19 pandemic has increased the number of deaths among those with AD [1]. Symptoms of AD/ADRD usually begin with Mild Cognitive Impairment (MCI) and include early onset memory loss, cognitive decline, and impairments with verbal language and visual/spatial perception. Approximately 12-18% of people age 60 or older are living with MCI in the U.S. Although older adults with MCI have the ability to independently perform most daily living activities such as eating, shopping, and bathing without help, the National Institute on Aging (NIA) estimated that 10 to 20% of subjects with MCI will develop dementia over a one-year period [2].

Magnetic Resonance Imaging (MRI) & Positron Emission Tomography (PET) scanning and neuropsychic examination are often used for identifying those with AD and dementia. These methods prove to be challenging for early MCI individuals given that the brain's structural changes and cognitive test results at this point might be harder to

differentiate from those with normal cognitive aging and the invasive nature of these assessments [3]. Using accurate, non-invasive, and cost-efficient diagnostic technology has the potential to bolster the early detection of MCI and AD. A 2019 study proposed that early detection of AD would decrease healthcare costs, and improve quality of life [4]. Studies have shown that MCI can affect the patterns of speech, language and face-to-face communication in older adults [5]. There are several studies on using traditional Machine Learning (ML) approaches such as Decision Tree [6, 7] and K-means clustering [7] to detect AD with human using collected demographic information [6] and MRI [7]. Other researchers used Cross-model Augmentation for automated detection of MCI from normal cognition (NC) using speech and language patterns [5]. However, there is fewer work on using ML models and particularly Deep Learning models for facial video analysis and then automated detection of MCI using visual features. This paper presents our recent work on developing and using Transformer-based models for the detection of MCI using facial videos collected in the Internet-Based Conversational Engagement Clinical Trial (I-CONECT) Study project¹ [8–10] (Clinicaltrials.gov #: NCT02871921). I-CONECT Study is a randomized controlled behavioral intervention trial aimed to enhance cognitive functions by providing frequent social interactions using video chats. Semi-structured 30-minutes conversations with interviewers were provided 4 times per week for 6 months to older adults. The study was funded by the National Institute on Aging (NIA).

Facial videos contain spatial features like facial expressions and head poses. It can also capture the facial expression change, track eye gaze motion, head pose movement,

*Corresponding author: Dr.Mohammad H. Mahoor
Tel: +1-303-871-3745 | Fax: +1-303-871-2194

✉ Jian.Sun86@du.edu (J. Sun);
hdodge@mgh.harvard.edu (H.H. Dodge);
mohammad.mahoor@du.edu (M.H. Mahoor)

🌐 <https://sites.google.com/view/sunjian/home> (J. Sun); <https://dodgelab.wixsite.com/dodge-lab> (H.H. Dodge); <http://mohammadmahoor.com> (M.H. Mahoor)
ORCID(s): 0000-0002-9367-0892 (J. Sun);
0000-0001-7290-8307 (H.H. Dodge); 0000-0001-8923-4660
(M.H. Mahoor)

¹Website: <https://www.i-conect.org/>.

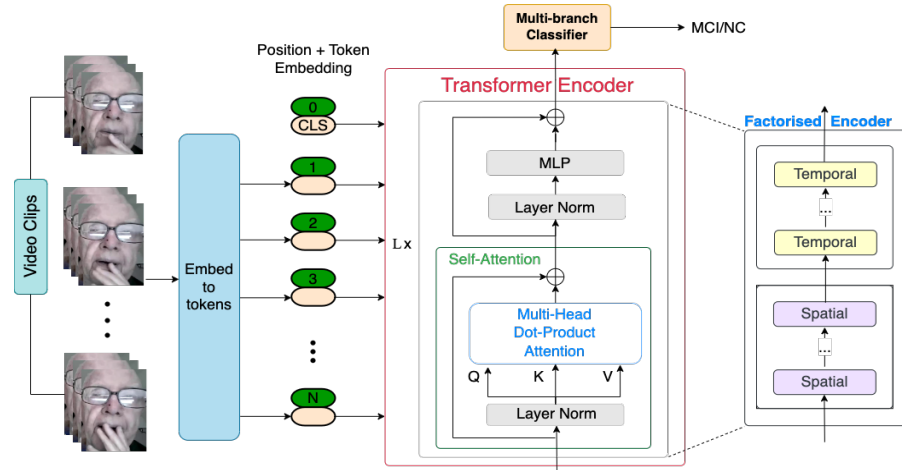


Figure 1: The structure of the proposed MC-ViT. It takes tubelet embedding to divide the video clips into cubes and loads these cubes into Transformer Encoder sequentially. Then, Transformer Encoder takes Factorised Encoder to extract spatio-temporal features. Finally, the output features go into Multi-branch Classifier to finish classification.

and lips activity, which are the temporal features and the key patterns in verbal and non-verbal communication [11, 12]. We hypothesize that facial videos collected during face-to-face communication in social settings can provide rich information for detection of MCI from NC subjects. To capture facial features out of facial videos, we develop a variant of Video Vision Transformer-based model (ViViT [13]). This model takes Vision Transformer (ViT) [14] as its backbone and captures spatio-temporal features. ViViT has proven its value on Facial Expression Recognition (FER) [15] and violence detection [16].

The I-CONECT dataset has both inter- and intra-class variations, which makes it a challenging video dataset. First, it is an imbalanced dataset as the distributions of MCI and NC subjects are uneven. This makes the dataset inter-class imbalance (aka Hard-Easy sample problem). The intra-class imbalanced issue happens within each class as the I-CONECT dataset consists of the videos in different lengths. Also, the quality of the videos in I-CONECT may vary from subject to subject. The occlusion and lightness problems in the videos decrease the quality of extracted spatio-temporal features. Furthermore, some subjects may not behave any symptoms of MCI, and act like NC in some video clips, which restricts ViViT from extracting enough MCI related features. This is so-called Positive-Negative sample problem.

To address these problems, we propose a Multi-branch Classifier (MC) module to augment representation capability of ViViT. The proposed MC has four levels of Fully Connected (FC) layers, where the third one has 4 branches. MC provides more features, but gives all features identical weight. Purely depending on MC contributes limitedly to the accuracy. We decide to assign different weights to features and class while computing loss. Subsequently, we combined Focal loss [17] and AD-CORRE loss [18] into the loss function for Hard-Easy and Positive-Negative Samples (HP loss) to relieve the negative effect of inter- and intra-class

imbalanced issues. Specifically, the Focal Loss is responsible for Hard-Easy sample problem, while AD-CORRE loss [18] handles Positive-Negative sample problem.

In summary, we present a new model called Multi-branch Classifier-ViT (MC-ViT), by integrating the aforementioned ViViT, MC, and HP Loss. We validated MC-ViT on several themes of the I-CONECT dataset. Our experimental results show that MC-ViT is highly capable to detect MCI from NC subjects.

The overall contributions are the summarized as follows:

- We propose MC-ViT to detect MCI from the interview videos provided by the I-CONECT Study.
- We design the MC module to enrich the extracted spatio-temporal features. Its multi-branch structure helps ViViT to capture the visual features from different perspectives.
- We develop the HP loss by combining Focal loss and AD-CORRE loss. The HP loss addresses the inter- and intra-class imbalanced issues and helps the model pay attention to classes with less samples and subjects with short video length.

The remainder of this paper is organized as follows. In Section 2, we discuss the previous works on analyzing and recognising facial expression and patterns of MCI people in videos using machine learning approaches. We also review the methods for augmenting features and handling Inter- and Intra-class imbalanced problems. Then, in Section 3, we present our new proposed model, including Tubelet Embedding, Factorised Encoder, Multi-branch Classifier, and HP Loss. Section 4 gives the details of our experiments including the dataset, data processing, evaluation metrics, implementation, results, discussion, and the ablation study. We finally conclude the paper with some suggestion for future research in Section 5.

2. Related Work

2.1. Detection of Mild Cognitive Impairment (MCI) Using Machine Learning Methods

Detection of MCI in older adults using innovative machine learning approaches has received great attention in the research community [19]. It is known that cognitive impairment and dementia adversely affect people's verbal and nonverbal behaviors, memory, cognitive functions, etc. Since the focus of this paper is on the detection of MCI using nonverbal visual patterns and behaviors expressed in facial videos of older adults using deep machine learning methods, we review the literature on using ML methods for detection of MCI. Some researchers have utilized traditional ML approaches to detect MCI or more advanced stages of cognitive impairment such as Alzheimer's disease and dementia. ML methods such as Support Vector Machines (SVM), Decision Trees, PCA+SVM, K-means cluster, hierarchical clustering, and Density-based spatial clusters of applications with noise (DBSCAN) [6, 7, 20–22] are the most common algorithms used in this domain.

Some researchers have exploited deep learning models to detect MCI and dementia, such as CNN models with Inception modules [23], linking a fully convolutional network (FCN) to a traditional multilayer perceptrons (MLP) [24], Inception-ResNet-V2 [25], and CNN-based models [22, 26–28].

Researchers have proposed that cognitive impairment and AD causes severe face recognition deficits and emotion detection deficits [29–35]. They collected the reaction of participants to specific emotions to estimate the degree of recognition deficits, which is a kind of MCI.

The aforementioned work did experiments on either brain Magnetic Resonance Imaging (MRI) scans, CT scans, and X-ray Scans [7, 20, 22, 23, 25–29, 36–38] or demographic information, patient interviews, and structured datasets that are available on line [6, 7, 20, 21, 24, 29–32, 34, 35, 39]. Collecting brain MRI and CT Scans are expensive. Other data modalities such as demographic information, patient interviews, and online structured datasets contain less complex, subtle, and subjective features. On the other hand, audiovisual collected during social interviews and face-to-face communication either in person or virtually contain rich verbal and nonverbal information.

Some researchers [11] video recorded the reaction of participants to different commands and introduced eye gaze and head pose in their study. Jiang *et al.* indicated the influence of eye-tracking on predicting cognitive impairment too [40]. Tanaka *et al.* filmed the video during the human-agent interaction and considered action units, eye gaze, and lip activity in the study [12]. It asked three fixed queries: Q1) What's the date today?, Q2) Tell me something interesting about yourself, Q3) How did you come here today? Then, Fei *et al.* argued that extracting facial features in dynamic approaches benefits analyzing the evolution of facial expressions and getting spatio-temporal

features [41]. It also showed different facial feature extraction techniques, such as Geometric, Appearance, Holistic, and Local. Finally, Umeda-Kameyama *et al.* explored the capability of Xception and other CNN-based models to distinguish between people with cognitive impairment and those without dementia [42]. Intuitively, our work explore the feasibility of an advanced deep learning model to predict MCI on the I-CONECT dataset.

2.2. Facial Video Analysis Using Deep Neural Models

Automated analysis of facial videos using deep machine learning and computer vision has been studied in the last decades. The applications vary from facial expression recognition (FER) [43–45], surveillance [46–48], pose estimation [49, 50], head gesture recognition [51? –54], medical applications [55–57], among others. This section presents related works that used deep neural network-based algorithms for facial video analysis.

When it comes to FER, some works used the traditional technique of converting videos into frames. For example, Liu *et al.* compressed videos into an apex frame by the encoding algorithm [58]. Jin *et al.* simply cut videos into images, but it enriched features by using facial landmark points [43]. Loading videos directly is another method. FER-GCN [44], TimeSformer [59], and three-stream network [60] simulated to analyze the video directly by taking multi frames as input. They stated that a sequence-based model helps extract temporal features. Based on multi frames, some researchers implemented a multi-frame optical flow method to get the difference between two frames [61, 62]. They claimed that multi-frame optical flow enriched temporal features. The aforementioned studies defended their idea with good experimental results. Furthermore, Jin *et al.* focused on diagnosing Parkinson's Disease (PD), which inspires us to believe that Deep Learning-based models are able to detect MCI [43].

Using more deep neural methods, Transformer-based models utilize modules to help capture spatio-temporal features in one stream, such as Convolutional Spatiotemporal Encoding layer from TimeConvNets [63] and Temporal Shift Module (TSM) from TimeSformer [59] and ViViT-B/16 \times 2 FE [13] (A ViT-Base backbone with a tubelet size of $h \times w \times t = 16 \times 16 \times 2$, FE represents factorized encoder). Other works utilized spatial-only attention and temporal-only attention consecutively to extract spatio-temporal features in one branch [59, 64, 65].

On the other hand, CNN-based models usually take multi-stream structure to extract spatio-temporal features separately, such as deep temporal-spatial networks [61], TMSAU-Net [62], and three-stream network [60]. These models take optical flow, frame difference, and motion vector methods to help create temporal information instead of learning from the raw images through the model. Models with 3D Convolutional operation can extract spatio-temporal information in one stream, but their large hyper-parameter scale improves computational complexity.

Comprehensively, to avoid the extra operation and implement the model thoroughly and efficiently, this research selected ViViT FE as the backbone of the proposed model.

2.3. Feature Enrichment using MLP Head

Inception Net [66] is a classic CNN model. It consists of repeated Inception Modules, which apply various scaled filters to extract features on the same layer and broad the network. The advantage of Inception Module is to enrich the features. Multi-models also helps augment representation and improve accuracy. Moreover, some researchers have shown the effect of multi-models on MCI detection [67–72]. In addition, a good Fully Connected layer benefits the model performance, such as XnODR and XnIDR [73]. The Inception Net and multi-models inspired the design of Multi-branch Classifier (MC) (see Section 3.3).

2.4. Inter-class and Intra-class Imbalanced Problems

Inter-class and intra-class imbalanced problems usually prevent ML model from predicting well. In [74] the authors explained that the inter-class imbalanced problem occurs when the number of samples in some classes is much larger than those in other classes, which causes the misclassification of rare class examples. The intra-class imbalanced dataset means that a class consists of several sub-concepts or sub-clusters. Moreover, at least one of the concepts or clusters is represented by the significantly less number of samples than the others [74]. The number of features from each sub-concept are unequal, which weakens the performance of classifier [75].

Focal Loss is powerful to equalize inter-class imbalanced datasets [17]. Moreover, classes with more features are easier to detect than those with less features. This is also called Hard-Easy sample problem. To address the intra-class imbalanced issue, researchers have proposed methods such as feature selection [74], resampling [74, 76, 76], and designing loss function [18, 77–79]. For example, EPIMTS (early prediction on the imbalanced multivariate time series) fused feature selection and resampling, which calls MUDSG to resample based on the extracted core shapelets [74]. Liu *et al.* utilized Soft Hard Example Mining (SHEM) to re-balance the error density distribution [76]. To achieve intra-class balancing, they assigned instance-wise sampling probabilities according to the prediction of the current ensemble model $F_{t-1}(\cdot)$ [76]. Other works focus on upgrading loss function. They proposed Discriminant Distribution-Agnostic loss (DDA loss) [77], Weighted Center Loss (WCL) [78], Deep Attentive Center Loss (DACL) [79], and Quadruplet loss [80]. These loss functions are tightly related to center loss. The goal of these methods is to achieve intra-class compactness and inter-class separation. The AD-CORRE loss presented in [18] aims to handle inter- and intra-class imbalanced issues, but it focuses on addressing the problem by digging the correlation between embeddings in the mini-batch level. Then, it embeds the influence of whole training samples into

batches incrementally instead of directly [18]. This has less computational cost.

In the I-CONECT dataset, the number of samples with MCI is apparently more than that with NC. Thus, subjects labeled in MCI are easy samples, while those labeled in NC are hard ones. To emphasize and increase the weight of NC, we apply Focal Loss to address the Hard-Easy sample problem.

Within each class, the number of frames from each video is unequal. In I-CONECT videos, the interviewees with MCI may behave normal cognitive sometime or show the symptom of MCI in one second. The proportion of normal and symptom parts is imbalanced and skewed too. For them, the normal acting parts are counted as negative samples, while the parts of MCI symptoms are positive samples. For subjects with NC, the definition of positive and negative samples is reversed. It is very important to draw a clear boundary between positive and negative samples instead of making them compact, even if classifying the normal sequence as NC decreases the prediction accuracy of subjects with MCI. In general, I-CONECT dataset has one inter-class imbalanced problem and two intra-class imbalanced problems. Based on the above discussion, we aim to achieve both inter- and intra-class separation, which is different from the target of the aforementioned loss functions such as DDA [77], WCL [78], and DACL [79]. To avoid suboptimal performance, after comprehensive thought, we are inclined to use the Adaptive Correlation (AD-CORRE) loss [18] to solve the Positive-Negative sample problem.

3. Multi-branch Classifier-ViViT (MC-ViViT)

The proposed Multi-branch Classifier-ViViT (MC-ViViT) is an end-to-end model, which predicts whether a video segment in the I-CONECT dataset belongs to the MCI group or normal cognition (NC). The backbone of the network is ViViT FE [13] as its Factorised Encoder structure can extract Spatio-Temporal features efficiently. To enrich the features and improve performance, MC-ViViT utilizes multi branches for classification. Specifically, MC-ViViT splits each video into several video cubes by Tubelet Embedding. Then, it embeds the video cubes into tokens and prepares the input tokens by concatenating class token and positional embedding. Subsequently, MC-ViViT applies the Transformer Encoder with Factorised Encoder to extract Spatio-Temporal features from the input tokens. Finally, the model computes the prediction score of each class using multi-branch classifiers. The rest of this section explains the model components in detail.

3.1. Tubelet Embedding Review

Following the pattern of ViViT [13], the cubic patch is non-overlapping too. Suppose that the tensor shape of one video clip is $[T, H, W, 3]$, where T is the frame numbers, H and W are the height and the width of each frame, 3 represents the RGB channels. Then, the tensor size of each cubic patch is $[t, h, w, 3]$. t , h , and w are the size of the corresponding temporal, height, and width dimensions. $n_t =$

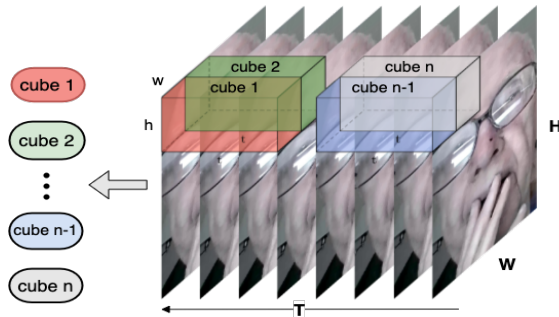


Figure 2: The structure of Tubelet Embedding.

$\lfloor \frac{T}{l} \rfloor^2$, $n_h = \lfloor \frac{H}{h} \rfloor$, and $n_w = \lfloor \frac{W}{w} \rfloor$ denote the token number of respective temporal, height, and width dimensions. The Tubelet Embedding changes the input unit from a 2D patch to a 3D cube, which contains temporal information (see Fig. 2). Therefore, it is the foundation of offering Spatio-Temporal information in MC-ViT.

3.2. Factorised Encoder (FE) Review

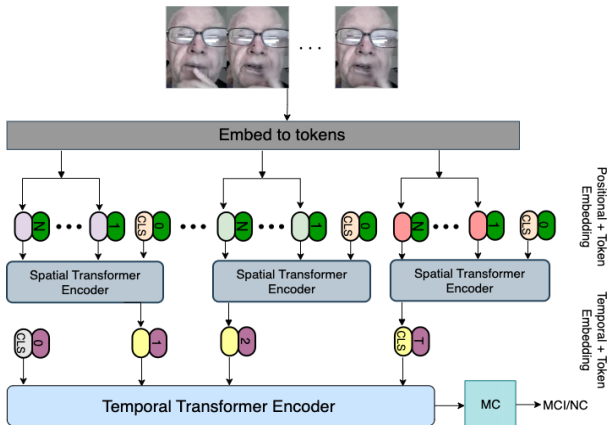


Figure 3: The structure of FE.

Fig. 1 shows that in ViViT [13], the Transformer Encoder takes the combined positional and embedded cubic tokens as input, and it contains Self-Attention module followed by the FeedForward module. Eq. 1 presents the details of the input tokens.

$$\mathbf{z} = [z_{cls}, \mathbf{Ex}_1, \mathbf{Ex}_2, \dots, \mathbf{Ex}_{n_h n_w n_t}] + \mathbf{p}, \quad (1)$$

where z_{cls} is a learnable class token, $[x_1, x_2, \dots, x_{n_h n_w n_t}]$ is the tensor of cubic patches, $x_i \in \mathbb{R}^{h \times w \times t}$, $n_h n_w n_t$ is the number of cubic patches. E is the linear projection to embed cubic patches. In addition, $\mathbf{p} \in \mathbb{R}^{n_h n_w n_t \times d}$ represents a learnable positional embedding. d is the dimension of the embedded token.

Given the layer l , the Self-Attention module consists of Layer Normalization (LN) and Multi-Head Dot-Product Attention, while the FeedForward (FF) module

² $\lfloor \cdot \rfloor$ means to get the largest integer not greater than \cdot .

includes LN and MLP. Both modules use skip-connection to enrich features and prevent gradient vanish. Moreover, Arnab *et al.* proposed four Multi-Head Self-Attention (MHSA) modules [13]. This work selected FE because Arnab *et al.* showed that ViViT FE performed the best of all four versions [13]. Fig. 3 shows that FE has two parts, Spatial Transformer Encoder (L_s) and Temporal Transformer Encoder (L_t). Spatial Transformer Encoder extracts latent representations on the different tokens with the same temporal index. Therefore, these latent representations are spatial features. Then, these latent representations with different temporal index come to the Temporal Transformer Encoder, which studies the interactions between tokens from different time steps. Thus, Temporal Transformer Encoder can mine temporal features. Assuming that the L_s and L_t repeats n_{sp} and n_{tp} times, respectively. FF processes the output of FE and returns Sequence-Level Spatio-Temporal feature. The above explanation can be summarized as Eqs. 2-5.

$$\mathbf{y}_s^l = L_{s_{n_{sp}}}^l (\dots L_{s_1}^l (LN(\mathbf{z}^l)) \dots) \quad (2)$$

$$\mathbf{y}_t^l = L_{t_{n_{tp}}}^l (\dots L_{t_1}^l (\mathbf{y}_s^l) \dots) \quad (3)$$

$$\mathbf{y}_{FE}^l = \mathbf{y}_t^l + \mathbf{z}^l \quad (4)$$

$$\mathbf{y}_{FF}^l = MLP(LN(\mathbf{y}_{FE}^l)) + \mathbf{y}_{FE}^l \quad (5)$$

3.3. Multi-branch Classifier (MC)

Inspired by Inception Module [66] and multi-models [67-72], MC takes multi-branch structure to provide different views and enrich representation as well. Different from Inception Module and multi-models, MC only does linear projection at each branch instead of convolutional operation or the neural network. In detail, MC consists of four FC layers. The dimension change is $64 \rightarrow 16 \rightarrow [8, 8, 8, 8] \rightarrow$ concatenate to $32 \rightarrow num_class$, where num_class represents the number of class. In our experiment, num_class is 2. When we convert the dimension from 16 to 32, Fig. 4 shows that we apply multi-branch structure to convert the dimension to 8 and repeat 4 times. Then, we concatenate them as a 32-dimensional tensor. With this structure, MC can provide more features and view the object from different angles.

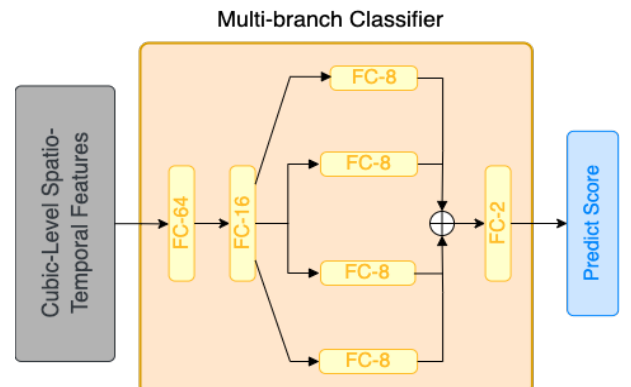


Figure 4: The structure of MC. \oplus represents concatenation.

3.4. Loss function for Hard-Easy and Positive-Negative Samples (HP Loss)

HP Loss has two components, Focal Loss [17] and AD-CORRE(FD) [18]. AD-CORRE(FD) is the FD (Feature Discriminator) component of AD-CORRE Loss.

3.4.1. Focal Loss Review

Focal Loss addresses the imbalance aspect of Hard-Easy samples by generating the weight based on sample numbers. It derives from α -balanced Cross Entropy loss. Then, adding a modulating factor $(1 - p_{mci})^\gamma$ defined in Eq. 7 to the cross entropy loss, with tunable focusing parameter $\gamma > 0$, makes the final Focal Loss. The above can be summarized as Eq. 6.

$$FL(p_{mci}) = -\alpha_{mci}(1 - p_{mci})^\gamma \log(p_{mci}) \quad (6)$$

where α is a weighting factor. $\alpha \in [0, 1]$ for class MCI and $1 - \alpha$ for class NC. p_{mci} represents the probability of the frame sequence attributing to MCI.

$$p_{mci} = \begin{cases} p & \text{if } y = MCI \\ 1 - p & \text{otherwise} \end{cases} \quad (7)$$

where p is the model's predict score, y is the predicted label.

3.4.2. AD-CORRE(FD) Review

AD-CORRE(FD) focuses on the correlation between the samples within a mini-batch. This prevents the imbalanced dataset from affecting the prediction. Therefore, the model pays attention to the class with less samples too. AD-CORRE(FD) comprises four key components of AD-CORRE(FD), Variance Eraser (Beta Matrix $\beta_{n \times n}$), Attention Map Matrix ($\Omega_{n \times n}$), Harmony Matrix ($\Phi_{n \times n}$), and Correlation Matrix (CORM). In short, AD-CORRE(FD) is a weighted mean absolute error and shown in Eq. 8.

$$FD = \frac{1}{kn^2} \sum_{l=0}^k \sum_{i=0}^n \sum_{j=0}^n \beta[i, j] \Omega[i, j] |\Phi[i, j] - CORM_l[i, j]|, \quad (8)$$

where k is the class number, n is the size of mini-batch. The difference between $\Phi_{n \times n}$ and $CORM_{n \times n}$ is the core of the AD-CORRE(FD) loss.

In general, AD-CORRE(FD) focuses on the correlation between samples within the mini-batch. This prevents the imbalanced dataset from affecting the prediction.

AD-CORRE(FD) Analysis

Intuitively, there are two ways to address the intra-class imbalance. Given a class, we assign trainable weight to each subject based on frame numbers. Or, we attribute different weights to positive and negative sequences within the same video. Either way, however, will stimulate more dispute and drive the problem complexity going exacerbation.

One this condition, AD-CORRE(FD)'s intention is to ignore the frames-imbalanced issue and the positive and

negative sample problem, and to only focus on the classification task in mini-batch level. The intervention of AD-CORRE(FD) avoids the deeper conflict. In addition, AD-CORRE(FD) substantially decreases the computation complexity because it only analyzes the similarity between embeddings within the mini-batch. It accumulatively collects class distribution information from previous batches to improve its adaptive weight. Calculating within the mini-batch is also the reason that AD-CORRE(FD) benefits on detecting minority samples.

3.4.3. Combine Two Loss Functions

Finally, Eq. 9 shows the HP Loss is the sum of Focal Loss and AD-CORRE (FD). We follow the pattern of AD-CORRE Loss and set λ as 0.5 as well.

$$HP\ Loss = FL(p_{mci}) + \lambda * AD\ - CORRE(FD) \quad (9)$$

4. Experiments

In this section, we first introduce the I-CONECT dataset, evaluation metrics, and implementation details. Then, we explain our experiments, present the results, report the ablation study, and evaluate the results.

4.1. Dataset

The Internet-Based Conversational Engagement Clinical Trial (I-CONECT) is to explore how social conversation can help improve memory and may prevent dementia or Alzheimer's disease in older adults. The study followed research participants aged 75 and older recruited from Portland, Oregon or Detroit, Michigan in the USA. The study randomized 187 participants. The participants had a 30-minute long chat per session with standardized interviewers (conversational staff) 4 times a week over a period of 6 months. The control group received only weekly 10-minutes phone check-ins. All participants connected with the conversational staff using study-provided user-friendly devices. Conversations were semi-structured with some standard prompts and daily topics, but once the conversation started, it flowed naturally for fun and engaging conversations. Out of 186 randomized participants, 86 participants are diagnosed as NC, while 101 people are diagnosed as MCI. In each 30 minutes-session, participants discussed one of the 161 selected themes, such as Summer Time, Health Care, Military Service, Television Technology, etc. The conversational interactions were recorded as videos. In the current study, we selected the following 4 themes: Crafts Hobbies, Day Time TV Shows, Movie Genres, and School Subjects. The interviewees talked about their crafts hobbies. They listed their favorite daytime TV shows, discussed preferred movie genres and showed example. Then, they also recalled their campus lives in School Subjects. Table 1 shows data exploration.

We used sequence-based approaches rather than frame-based approaches to process the dataset, and extracted facial features via a dynamic approach.

Table 1

The details of researched themes. Subject Number is the total number of videos in the corresponding theme. Male/Female and MCI/NC shows the gender distribution and category distribution. Frame Number is the total image number of each theme after converting videos into frames.

	Crafts Hobbies	Day Time TV Shows	Movie Genres	School Subjects
Subject Number	32	41	35	39
Male/Female	11/21	11/30	10/25	11/28
MCI/NC	20/12	20/21	21/14	22/17
Frame Number	691872	859872	770656	797968

4.2. Data Processing

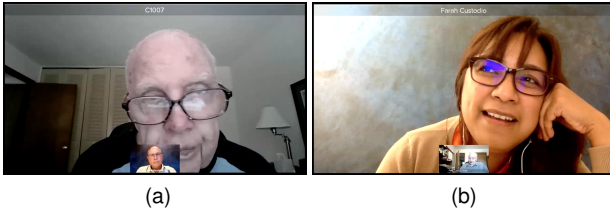


Figure 5: Two sample frames from the video dataset. In (a), the window of interviewee is bigger than that of interviewer because interviewer was speaking. Conversely, in (b), interviewer was talking so that her window is bigger than interviewee's.

The facial features of interviewees are valuable to our research. Usually, subject talks like NC at the start and the end, which prevents the model from predicting accurately. Furthermore, Fig. 5 shows that every video has a complex background and interviewers' faces, which has a negative influence on predicting results. To address this problem, we decide to drop the first 3 minutes and the last 2.5 minutes of each video. Then, EasyOCR helps detect whether or not the upper half frame contains the subject ID in the given frame. For frames with the subject ID on the top, we implemented RetinaFace [81] to crop the participants' facial images and dropped all irrelevant and interfering information. In detail, we calculate the area of detected faces and the Intersection over Union (IoU) of them. If $\text{IoU} < 0.05$, we kept the bigger face like Fig. 5a. Otherwise, we continue to process the next frame and drop the frame like Fig. 5b. Finally, we browse the kept images and manually delete the wrongly saved ones. We used this method to process different themes.

Albeit, there are in total of 70 participants, each theme may contain videos less than 40. For the sake of taking advantage of videos thoroughly and predicting better, we select K-fold Cross Validation and use Eq. 10 to calculate K for each theme.

$$K = \lfloor N_{\text{Video}} / L_{\text{Fold}} \rfloor \quad (10)$$

where N_{Video} and L_{Fold} are the video number of selected theme and that of each fold. We set $L_{\text{Fold}} = 3$ in our study. Moreover, videos in each fold belong to different participants.

Simultaneously, inspired by [44, 59, 60, 63], this study used multi frames as the input. Thus, we cut each video

Table 2

The prediction accuracy of detecting MCI on 4 themes using K-fold evaluation.

Test Theme	Crafts Hobbies	Day Time TV Shows	Movie Genres	School Subjects
Fold Num	11	14	11	13
Accuracy	29/32	36/41	30/35	35/39
	90.63%	85.37%	85.71%	89.74%
F1	93.03%	85.00%	88.37%	90.47%
AUC	0.6042	0.4952	0.6122	0.5294
MCI/NC	20/12	20/21	21/14	22/17
Sensitivity/ Specificity	100%/ 75%	85%/ 85.71%	90.48%/ 78.57%	86.36%/ 94.12%

into a certain number of fixed-length segments as inputs. Let L^3 be the number of consecutive frames in a divided segment, N represents the number of total frames. $\lfloor N / L \rfloor$ is the number of segments for each video.

4.3. Evaluation Metrics

Prediction accuracy, F1 score, AUC (Area Under the Receiver Operating Characteristic Curve), Sensitivity, and Specificity are the evaluation metrics in the experiment. McNamara and Martin stated that sensitivity and specificity are intrinsic measures of a case definition or diagnostic test, whereas predictive values vary with the prevalence of a condition within a population [82]. Eq. 11 presents the statistical definition of sensitivity, which is similar to recall. Eq. 12 is the equation of specificity.

$$\text{Sensitivity} = \frac{\text{True Positive}}{\text{True Positive} + \text{False Negative}} \quad (11)$$

$$\text{Specificity} = \frac{\text{True Negative}}{\text{True Negative} + \text{False Positive}} \quad (12)$$

4.4. Implementation Details

We performed data augmentation to each segment, which contains the random horizontal and vertical flip, random rotation, and center crop. All frames within one set do exactly same augmentation. The batch size is 80. Following the pattern of [44, 59, 60, 63], L is 16. The initialized learning rate is 1e-6. We used Adam optimizer and Cyclic scheduler with the mode of triangular2. The loss function is HP loss. The epoch number is 30. We coded the network by PyTorch 1.12.0+cu116 and ran experiments on the NVIDIA GTX 1080Ti GPU.

To completely evaluate the new proposed architecture, we designed three experiments (See Sections 4.5 - 4.7).

4.5. Experiment: K-fold Validation

This experiment is to test the capability of MC-ViT on predicting MCI in each theme. The inputs are all the corresponding videos.

We report the results in Table 2. MC-ViT achieves over 85% accuracy on all four themes. For example, MC-ViT predicts 29 out of 32 subjects correctly on the

³ L and T from Section 3.1 are identical.

Table 3

The prediction accuracy a cross-theme fashion. Three themes are used for training a model and the left theme is used for test.

Test Theme	Crafts Hobbies	Day Time TV Shows	Movie Genres	School Subjects
Fold Num	11	14	11	10
Accuracy	27/32	33/41	30/35	32/39
	84.38%	80.49%	85.71%	82.05%
F1	87.80%	82.61%	88.89%	89.36%
AUC	0.7	0.7452	0.6701	0.4773
MCI/NC	20/12	20/21	21/14	22/17
Sensitivity/ Specificity	90%/ 75%	95%/ 66.67%	95.24%/ 71.43%	95.45%/ 76.47%

theme Crafts Hobbies, which reaches the highest accuracy, 90.63%. The accuracy of School Subjects is 89.74%, which is close to 90%. Three of the F1 Scores are more than 88%, and only the F1 score of Day Time TV Shows is 85%. The accuracy and F1 Score solidly support that MC-ViViT has robust performance. The other evidence comes from AUC Score. The average AUC of all four themes is 0.56. Given that not all the clips have MCI features in the video, even for subjects with MCI, it is reasonable to predict parts of their video sequences as NC. Due to this reason, some subjects will be correctly predicted as MCI with low scores. Thus, the average AUC value is around 0.6.

Table 2 also shows that, on all four themes, MCI/NC has related balanced prediction distribution. Their Sensitivity and Specificity are high as well. For instance, the sample of Day Time TV Shows comprise 20 MCI subjects and 21 NC ones. The Sensitivity over Specificity is 85%/85.71%.

4.6. Experiment: cross themes evaluation

This experiment is to test if MC-ViViT can integrate and learn complex features from a given set of training themes and detect MCI from different test themes correctly. We train the video on three themes and predict the rest one. This time, we resize all the frames as 96×96 to train faster. There are not overlapped subjects between the training sets and the test sets.

Table 3 shows all the results. MC-ViViT still provides stable performance. It achieves over 82% accuracy and over 87% F1 Score on the three themes. The highest accuracy is 85.71% (predict 30 out of 35 samples correctly) on the Movie Genres, while the highest F1 Score is 89.36% on the School Subject. The accuracy and F1 Score of this experiment are still robust to show that MC-ViViT can predict well. The average AUC Score of this experiment is 0.648, which is higher than 0.56 from Section 4.5. This value also accords to the analysis from Section 4.5. It supports that MC-ViViT can make objective decision. In the meanwhile, MC-ViViT only reaches 80.49% accuracy and 82.61% F1 Score on the Day Time TV Shows. This is due to the smaller frame size.

Subsequently, Table 2 presents that, the smaller frame size affects the Sensitivity over Specificity of MCI/NC. In specific, it weakens the capability of detecting negative samples, which is NC in our experiment. Thereby, the

Table 4

The prediction accuracy on 4 themes with different t size.

Test Theme	Crafts Hobbies	Day Time TV Shows	Movie Genres	School Subjects
$t = 2$	84.38%	58.54%	82.86%	71.79%
$t = 4$	90.63%	85.37%	85.71%	89.74%
$t = 8$	81.25%	75.61%	85.71%	76.92%

Table 5

The prediction accuracy on 4 themes with or without MC. No multi-branch means that we drop the multi branches during the experiment.

Test Theme	Crafts Hobbies	Day Time TV Shows	Movie Genres	School Subjects
MC	90.63%	85.37%	85.71%	89.74%
No MC	78.13%	63.41%	74.29%	74.36%

results of Sensitivity/Specificity are less balance than those from Section 4.5. For example, the Sensitivity/Specificity of movie genres increases from 90.48%/78.57% (Table 2) to 95.24%/71.43%. Smaller frame size decreasing the important features of NC makes the NC more harder to detect. Therefore, Specificity in this experiment is lower than Section 4.5.

4.7. Ablation Study

This section discusses the effect of temporal dimension t , MC, and HP Loss on the performance of MC-ViViT (Sections 4.7.1-4.7.3).

4.7.1. Study the most proper temporal dimension t

In MC-ViViT, the frame number, T , is 16, which can be divided by $[1, 2, 4, 8, 16]$. To keep Tubelet Embedding and reduce the burden of computation, we set the temporal dimension t as $[2, 4, 8]$ alternatively to study the best value for this research.

Table 4 shows that the $t = 4$ predicts the best under the current configuration on four themes. Therefore, we set the $t = 4$.

4.7.2. Study the effect of MC

This study is to evaluate the effect of MC structure. In the experiment, we dropped the multi-branch structure and changed the dimension from 16 to num_class directly. The dimension changes will be $64 \rightarrow 16 \rightarrow num_class$. We collected the related experimental results in Table 5. It shows that, for each theme, the accuracy of ViViT with MC is at least 10% higher than that without MC. Therefore, MC module provides more features and benefits the ViViT on predicting better.

4.7.3. Study the effect of HP Loss

This study is to test the influence of each component of HP Loss on the prediction. We firstly did experiments with Focal Loss only. Then, we did experiments with AD-CORRE(FD) Loss only. Table 6 contains all the results and

Table 6

The prediction accuracy on 4 themes with different loss function.

Test Theme	Crafts Hobbies	Day Time TV Shows	Movie Genres	School Subjects
HP Loss	90.63%	85.37%	85.71%	89.74%
Focal Loss	68.75%	68.29%	68.57%	66.67%
AD-CORRE(FD)	53.13%	60.98%	60.00%	56.41%

shows that MC-ViViT using Focal loss performs better than that using AD-CORRE(FD). In the meanwhile, the accuracy of MC-ViViT using HP loss surpasses at least 14% than that using either Focal loss or AD-CORRE(FD). Thereby, Table 6 upholds that HP Loss helps the MC-ViViT perform better than each individual component does.

5. Discussion

The experiments presented in Sections 4.5 and 4.6 indicate that MC-ViViT can detect MCI with a promising accuracy. For a selected theme, MC-ViViT can predict subjects not included in the model training very well. It can also infer the representations learned from many themes to correctly predict the subjects from unseen themes. The model has a robust performance, which convinces us that analyzing semi-structured interview videos is useful to detect MCI.

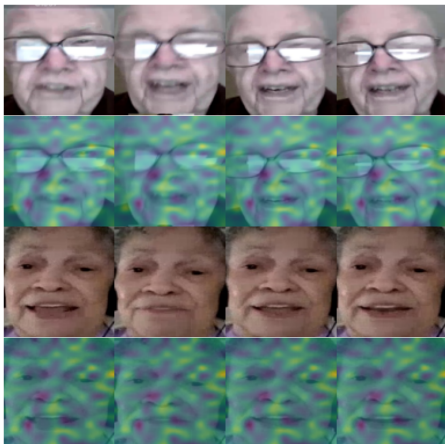


Figure 6: The extracted spatio-temporal feature maps on 16 consecutive frames from two subjects. MC-ViViT focuses more on the bright areas and pays less attention on the dark ones. Given that there are n_t tubelets, where $n_t = \lfloor \frac{T}{t} \rfloor = \lfloor \frac{16}{4} \rfloor = 4$, there are four feature maps. To simplify the visualization, we pick the first frame of each tubelet to represent it.

In the meanwhile, ViViT, as the backbone, mainly provides good representations to the final prediction. These good representations include spatial features and temporal ones. Different from manually described and learned pattern such as head pose, eye gaze, eye-tracking, and lip activities, Fig. 6 shows that MC-ViViT pays attention on the different areas of the face. For example, it focuses on regions of the forehead, eyelids, nose, cheek, and jaw. This correlates with the statement that ViViT is capable to monitor the motion of all facial muscles and discover many slight changes and

features. Furthermore, Sections 4.5 and 4.6 indicate that these features are very important to decide if the subject has MCI or not. In short, ViViT takes video clips as the input and extracts spatio-temporal features in one stream, which enables the model to make a comprehensive decision. Subsequently, the ablation study from Section 4.7 suggests that both MC and HP Loss improve the accuracy. MC broadens the network by the multi-branch structure, which provides different perspective to analyze the subject's features. MC strengthens the features' richness, which benefits on making correct decision. HP Loss, then, concentrates on the prediction equality. I-CONECT dataset is a very imbalanced dataset. Table 1 indicates that every theme has more MCI subjects than NC ones. Focal Loss part of HP loss assigns more weights to the class with less subjects, and aims to solve inter-class imbalanced issue. Within each class, the different video length causes the inequivalence of extracted frames from each subject. The AD-CORRE(FD) part of HP Loss changes the background of problem from the intra-class level to mini-batch level. Within the mini-batch, AD-CORRE(FD) tackles the classification task by measuring the similarity between embedding features, which wisely resolves the imbalance crisis and reduces the computational complexity. Thereby, HP loss is essential to the MC-ViViT. The experimental results from Tables 5 and 6 uphold the above discussion. In addition, Table 2 indicates that MC-ViViT can learn features well under one particular theme, while Table 3 convinces us that features from other themes can help detect MCI from NC on the left one. Subjects perform similar features on the different themes.

In general, there are two key findings. The first one is that Transformer-based models are capable to detect MCI on the early stage only by analyzing facial features; the second one is that semi-structured interview videos can provide plenty of features to help model make quality prediction while merely requires the tablet computer or mobile phone to collect. This costs much less than collecting conventional medical images like MRI. These two findings reveal that MC-ViViT has potential to detect other diseases, such as dementia and Parkinson's Disease (PD), on the early stage. Moreover, the corresponding data collection becomes convenient and easy to access. Even a cell phone can help film facial videos.

On the other side, due to the lack of consistent video recording environment, the videos' qualities vary a lot. From what we observed in this research, the video quality significantly affects the prediction. We notice that MC-ViViT usually predicts high clarity videos rightly with high prediction scores. Conversely, MC-ViViT is easy to give vague videos a low prediction scores. Or even MC-ViViT classifies vague videos to wrong labels. This explains the reason that Sensitivity versus Specificity is far from equivalence. The future work will focus on establishing a mechanism to evaluate the video quality score. The future model will implement this score to design a new loss function which helps tune the training process.

6. Conclusion

This paper presented MC-ViT to detect MCI from NC via facial videos of the semi-structured interviews (I-CONECT dataset). The experiments show that MC-ViT can predict well with the help of MC and HP Loss. Simultaneously, it shows that the Transformer-based model can tell whether or not people have MCI merely by analyzing facial features from the semi-structured interview videos. Compared to the other datasets mentioned in Section 1, I-CONECT dataset is easy to access, low cost, time-saving, flexible, and less restricted. It is very valuable to spread and propagate.

Acknowledgement

We would like to thank Miss. Jisu Lee for proofreading this paper.

Author Contributions

Jian Sun: Conceptualization, Methodology, Software, Validation, Formal analysis, Investigation, Data Curation, Writing - Original Draft, Writing - Review & Editing, Visualization.

Hiroko Hayama Dodge: Investigation, Resources, Data Curation, Writing—Review and Editing.

Mohammad H. Mahoor: Resources, Writing—Review and Editing, Supervision, Project Administration.

References

[1] A. Association, 2021 alzheimer's disease facts and figures, *Alzheimer's & Dementia* 17 (2021) 327–406.

[2] N. I. on Aging, What is mild cognitive impairment?, 2021. URL: <https://www.nia.nih.gov/health/what-mild-cognitive-impairment>.

[3] F. Tang, I. Uchendu, F. Wang, H. H. Dodge, J. Zhou, Scalable diagnostic screening of mild cognitive impairment using ai dialogue agent, *Alzheimer's & Dementia* 16 (2020).

[4] W. S. Eikelboom, E. Singleton, E. Van Den Berg, M. Coesmans, F. Mattace Raso, R. L. Van Bruchem, J. A. Goudzwaard, F. J. De Jong, M. Koopmanschap, T. Den Heijer, et al., Early recognition and treatment of neuropsychiatric symptoms to improve quality of life in early alzheimer's disease: protocol of the beat-it study, *Alzheimer's research & therapy* 11 (2019) 1–12.

[5] G. Liu, Z. Xue, L. Zhan, H. H. Dodge, J. Zhou, Detection of mild cognitive impairment from language markers with crossmodal augmentation, in: PACIFIC SYMPOSIUM ON BIOCOMPUTING 2023: Kohala Coast, Hawaii, USA, 3–7 January 2023, World Scientific, 2022, pp. 7–18.

[6] J. Neelaveni, M. Devasana, Alzheimer disease prediction using machine learning algorithms, in: 2020 6th International Conference on Advanced Computing and Communication Systems (ICACCS), 2020, pp. 101–104. doi:[10.1109/ICACCS48705.2020.9074248](https://doi.org/10.1109/ICACCS48705.2020.9074248).

[7] R. Davuluri, R. Rengaswamy, A survey of different machine learning models for alzheimer disease prediction, *International Journal of Emerging Trends in Engineering Research* 8 (2020).

[8] D. Carr, How to successfully navigate a revise-and-resubmit decision and handle rejections, *Innovation in Aging* 3 (2019) S224.

[9] C.-Y. Wu, N. Mattek, K. Wild, L. M. Miller, J. A. Kaye, L. C. Silbert, H. H. Dodge, Can changes in social contact (frequency and mode) mitigate low mood before and during the covid-19 pandemic? the i-connect project, *Journal of the American Geriatrics Society* 70 (2022) 669–676.

[10] K. Yu, K. Wild, K. Potempa, B. M. Hampstead, P. A. Lichtenberg, L. M. Struble, P. Pruitt, E. L. Alfaro, J. Lindsley, M. MacDonald, et al., The internet-based conversational engagement clinical trial (i-connect) in socially isolated adults 75+ years old: randomized controlled trial protocol and covid-19 related study modifications, *Frontiers in digital health* 3 (2021) 714813.

[11] U. Nam, K. Lee, H. Ko, J.-Y. Lee, E. C. Lee, Analyzing facial and eye movements to screen for alzheimer's disease, *Sensors* 20 (2020).

[12] H. Tanaka, H. Adachi, H. Kazui, M. Ikeda, T. Kudo, S. Nakamura, Detecting dementia from face in human-agent interaction, *Adjunct of the 2019 International Conference on Multimodal Interaction* (2019).

[13] A. Arnab, M. Dehghani, G. Heigold, C. Sun, M. Lučić, C. Schmid, Vivit: A video vision transformer, in: *Proceedings of the IEEE/CVF International Conference on Computer Vision*, 2021, pp. 6836–6846.

[14] A. Dosovitskiy, L. Beyer, A. Kolesnikov, D. Weissenborn, X. Zhai, T. Unterthiner, M. Dehghani, M. Minderer, G. Heigold, S. Gelly, J. Uszkoreit, N. Houlsby, An image is worth 16x16 words: Transformers for image recognition at scale, *ArXiv* abs/2010.11929 (2020).

[15] Z. Huang, Z. Qing, X. Wang, Y. Feng, S. Zhang, J. Jiang, Z. Xia, M. Tang, N. Sang, M. H. Ang Jr, Towards training stronger video vision transformers for epic-kitchens-100 action recognition, *arXiv preprint arXiv:2106.05058* (2021).

[16] S. Singh, S. Dewangan, G. S. Krishna, V. Tyagi, S. Reddy, Video vision transformers for violence detection, *arXiv preprint arXiv:2209.03561* (2022).

[17] T.-Y. Lin, P. Goyal, R. Girshick, K. He, P. Dollár, Focal loss for dense object detection, in: *Proceedings of the IEEE international conference on computer vision*, 2017, pp. 2980–2988.

[18] A. P. Fard, M. H. Mahoor, Ad-corre: Adaptive correlation-based loss for facial expression recognition in the wild, *IEEE Access* 10 (2022) 26756–26768.

[19] S. Cavedoni, A. Chirico, E. Pedroli, P. Cipresso, G. Riva, Digital biomarkers for the early detection of mild cognitive impairment: artificial intelligence meets virtual reality, *Frontiers in Human Neuroscience* 14 (2020) 245.

[20] Y. Asim, B. Raza, A. K. Malik, S. Rathore, L. Hussain, M. A. Iftikhar, A multi-modal, multi-atlas-based approach for alzheimer detection via machine learning, *International Journal of Imaging Systems and Technology* 28 (2018) 113–123.

[21] Y. Pang, W. Kukull, M. Sano, R. Albin, C. Shen, J. Zhou, H. Dodge, Predicting progression from normal to mci and from mci to ad using clinical variables in the national alzheimer's coordinating center uniform data set version 3: Application of machine learning models and a probability calculator, *The journal of prevention of Alzheimer's disease* (2023).

[22] L. J. C. de Mendonça, R. J. Ferrari, A. D. N. Initiative, et al., Alzheimer's disease classification based on graph kernel svms constructed with 3d texture features extracted from mr images, *Expert Systems with Applications* 211 (2023) 118633.

[23] Y. Ding, J. H. Sohn, M. G. Kawczynski, H. Trivedi, R. Harnish, N. W. Jenkins, D. Lituiev, T. P. Copeland, M. S. Aboian, C. Mari Aparici, S. C. Behr, R. R. Flavell, S.-Y. Huang, K. A. Zalocusky, L. Nardo, Y. Seo, R. A. Hawkins, M. Hernandez Pampaloni, D. Hadley, B. L. Franc, A deep learning model to predict a diagnosis of alzheimer disease by using 18f-fdg pet of the brain, *Radiology* 290 (2019) 456–464. PMID: 30398430.

[24] S. Qiu, P. Joshi, M. I. Miller, C. Xue, X. Zhou, C. Karjadi, G. H. Chang, A. S. Joshi, B. Dwyer, S. Zhu, M. C. Kak, Y. Zhou, Y. J. Alderazi, A. Swaminathan, S. Kedar, M. Saint-Hilaire, S. H. Auerbach, J. Yuan, E. Sartor, R. Au, V. B. Kolachalam, Development and validation of an interpretable deep learning framework for alzheimer's disease classification, *Brain* 143 (2020) 1920 – 1933.

[25] B. Lu, H.-X. Li, Z.-K. Chang, L. Li, N.-X. Chen, Z.-C. Zhu, H.-X. Zhou, X.-Y. Li, Y.-W. Wang, S.-X. Cui, Z.-Y. Deng, Z. Fan, H. Yang,

X. Chen, P. M. Thompson, F. X. Castellanos, C.-G. Yan, for the Alzheimer's Disease Neuroimaging Initiative, A practical alzheimer disease classifier via brain imaging-based deep learning on 85,721 samples, *bioRxiv* (2021).

[26] A. W. Salehi, P. Baglat, B. B. Sharma, G. Gupta, A. Upadhyay, A cnn model: Earlier diagnosis and classification of alzheimer disease using mri, in: 2020 International Conference on Smart Electronics and Communication (ICOSEC), 2020, pp. 156–161. doi:[10.1109/ICOSEC49089.2020.9215402](https://doi.org/10.1109/ICOSEC49089.2020.9215402).

[27] K. M. Poloni, R. J. Ferrari, A. D. N. Initiative, et al., A deep ensemble hippocampal cnn model for brain age estimation applied to alzheimer's diagnosis, *Expert Systems with Applications* 195 (2022) 116622.

[28] A. De, A. S. Chowdhury, Dti based alzheimer's disease classification with rank modulated fusion of cnns and random forest, *Expert Systems with Applications* 169 (2021) 114338.

[29] C. Mazzi, G. Massironi, J. Sanchez-Lopez, L. De Togni, S. Savazzi, Face recognition deficits in a patient with alzheimer's disease: Amnesia or agnosia? the importance of electrophysiological markers for differential diagnosis, *Frontiers in Aging Neuroscience* 12 (2020).

[30] M. Martinez, N. Multani, C. J. Anor, K. Misquitta, D. F. Tang-Wai, R. Keren, S. Fox, A. E. Lang, C. Marras, M. C. Tartaglia, Emotion detection deficits and decreased empathy in patients with alzheimer's disease and parkinson's disease affect caregiver mood and burden, *Frontiers in Aging Neuroscience* 10 (2018).

[31] B. T. M. de Melo Fádel, R. L. S. D. Carvalho, T. T. B. A. D. Santos, M. C. N. Dourado, Facial expression recognition in alzheimer's disease: A systematic review, *Journal of Clinical and Experimental Neuropsychology* 41 (2018) 192–203.

[32] M. Dourado, B. Fdel, J. Neto, G. Alves, C. Alves, Facial expression recognition patterns in mild and moderate alzheimer's disease, *Journal of Alzheimer's Disease* 69 (2019) 1–11.

[33] J. C. Meléndez, E. Satorres, I. Oliva, Comparing the effect of interference on an emotional stroop task in older adults with and without alzheimer's disease, *Journal of Alzheimer's disease : JAD* 73 (2020) 1445–1453.

[34] R. Gil, E. M. Arroyo-Anllá, Alzheimer's disease and face masks in times of covid-19, *Journal of Alzheimer's disease : JAD* 79 (2021) 9–14.

[35] L.-A. Sapey-Triomphe, R. A. Heckemann, N. Boublay, J.-M. Dorey, M. A. Hénaff, I. Rouch, C. Padovan, A. Hammers, P. Krölik-Salmon, Neuroanatomical correlates of recognizing face expressions in mild stages of alzheimer's disease, *PLoS ONE* 10 (2015).

[36] J. Islam, Y. Zhang, Early diagnosis of alzheimer's disease: A neuroimaging study with deep learning architectures, in: 2018 IEEE/CVF Conference on Computer Vision and Pattern Recognition Workshops (CVPRW), 2018, pp. 1962–19622. doi:[10.1109/CVPRW.2018.00247](https://doi.org/10.1109/CVPRW.2018.00247).

[37] R. Rehouma, M. Buchert, Y.-P. P. Chen, Machine learning for medical imaging-based covid-19 detection and diagnosis, *International Journal of Intelligent Systems* 36 (2021) 5085–5115.

[38] M.-A. Mercioni, L. L. Stavarache, Disease diagnosis with medical imaging using deep learning, in: K. Arai (Ed.), *Advances in Information and Communication*, Springer International Publishing, Cham, 2022, pp. 198–208.

[39] M. Hammoudeh, U. Nagavelli, D. Samanta, P. Chakraborty, Machine learning technology-based heart disease detection models, *Journal of Healthcare Engineering* 2022 (2022).

[40] Z. Jiang, S. Seyed, R. U. Haque, A. L. Pongos, K. L. Vickers, C. M. Manzanares, J. J. Lah, A. I. Levey, G. D. Clifford, Automated analysis of facial emotions in subjects with cognitive impairment, *PLOS ONE* 17 (2022) 1–19.

[41] Z. Fei, E. Yang, D. D.-U. Li, S. Butler, W. Ijomah, H. Zhou, A survey on computer vision techniques for detecting facial features towards the early diagnosis of mild cognitive impairment in the elderly, *Systems Science & Control Engineering* 7 (2019) 252–263.

[42] Y. Umeda-Kameyama, M. Kameyama, T. Tanaka, B.-K. Son, T. Kojima, M. Fukasawa, T. Iizuka, S. Ogawa, K. Iijima, M. Akishita, Screening of alzheimer's disease by facial complexion using artificial intelligence, *Aging* 13 (2021) 1765–1772.

[43] B. Jin, Y. Qu, L. Zhang, Z. Gao, Diagnosing parkinson disease through facial expression recognition: Video analysis, *J Med Internet Res* 22 (2020) e18697.

[44] D. Liu, H. Zhang, P. Zhou, Video-based facial expression recognition using graph convolutional networks, 2020 25th International Conference on Pattern Recognition (ICPR) (2021) 607–614.

[45] S. Khan, G. Xu, R. Chan, H. Yan, An online spatio-temporal tensor learning model for visual tracking and its applications to facial expression recognition, *Expert Systems with Applications* 90 (2017) 427–438.

[46] D. R. Patrikar, M. R. Parate, Anomaly detection using edge computing in video surveillance system, *International Journal of Multimedia Information Retrieval* 11 (2022) 85–110.

[47] X. Ling, J. Liang, D. Wang, J. Yang, A facial expression recognition system for smart learning based on yolo and vision transformer, in: 2021 7th International Conference on Computing and Artificial Intelligence, ICCAI 2021, Association for Computing Machinery, New York, NY, USA, 2021, p. 178–182. URL: <https://doi.org/10.1145/3467707.3467733>. doi:[10.1145/3467707.3467733](https://doi.org/10.1145/3467707.3467733).

[48] Y. Song, H. Tang, F. Meng, C. Wang, M. Wu, Z. Shu, G. Tong, A transformer-based low-resolution face recognition method via on-and-offline knowledge distillation, *Neurocomputing* 509 (2022) 193–205.

[49] H. Liu, S. Fang, Z. Zhang, D. Li, K. Lin, J. Wang, Mfdnet: Collaborative poses perception and matrix fisher distribution for head pose estimation, *IEEE Transactions on Multimedia* 24 (2022) 2449–2460.

[50] O. Sümer, P. Goldberg, S. D'Mello, P. Gerjets, U. Trautwein, E. Kasneci, Multimodal engagement analysis from facial videos in the classroom, *IEEE Transactions on Affective Computing* (2021) 1–1.

[51] A. R. Khan, T. Saba, M. Z. Khan, S. M. Fati, M. U. G. Khan, Classification of human's activities from gesture recognition in live videos using deep learning, *Concurrency and Computation: Practice and Experience* 34 (2022) e6825.

[52] S. Gashi, A. Saeed, A. Vicini, E. Di Lascio, S. Santini, Hierarchical classification and transfer learning to recognize head gestures and facial expressions using earbuds, in: Proceedings of the 2021 International Conference on Multimodal Interaction, 2021, pp. 168–176.

[53] J. Li, S. Xu, X. Qin, A hierarchical model for learning to understand head gesture videos, *Pattern Recognition* 121 (2022) 108256.

[54] J. Xia, H. Zhang, S. Wen, S. Yang, M. Xu, An efficient multitask neural network for face alignment, head pose estimation and face tracking, *Expert Systems with Applications* 205 (2022) 117368.

[55] B. Sonawane, P. Sharma, Review of automated emotion-based quantification of facial expression in parkinson's patients, *The Visual Computer* 37 (2021) 1151–1167.

[56] K. G. Sibley, C. Girges, E. Hoque, T. Foltyne, Video-based analyses of parkinson's disease severity: A brief review, *Journal of Parkinson's disease* 11 (2021) S83–S93.

[57] A. Villa, V. Sankar, C. Shibusaki, Tele (oral) medicine: A new approach during the covid-19 crisis, *Oral Diseases* 27 (2021) 744.

[58] X. Liu, L. Jin, X. Han, J. You, Mutual information regularized identity-aware facial expression recognition in compressed video, *Pattern Recognition* 119 (2021) 108105.

[59] B. Mohan, M. Popa, Temporal based emotion recognition inspired by activity recognition models, in: 2021 9th International Conference on Affective Computing and Intelligent Interaction Workshops and Demos (ACIIW), 2021, pp. 01–08. doi:[10.1109/ACIIW52867.2021.9666356](https://doi.org/10.1109/ACIIW52867.2021.9666356).

[60] J.-H. Kim, N. Kim, C. S. Won, Facial Expression Recognition with Swin Transformer, *arXiv e-prints* (2022) arXiv:2203.13472.

[61] X. Pan, S. Zhang, W. Guo, X. Zhao, Y. Chuang, Y. Chen, H. Zhang, Video-based facial expression recognition using deep temporal-spatial networks, *IETE Technical Review* 37 (2020) 402–409.

[62] L. Liang, C. Lang, Y. Li, S. Feng, J. Zhao, Fine-grained facial expression recognition in the wild, *IEEE Transactions on Information Forensics and Security* 16 (2021) 482–494.

[63] J. R. Hou Lee, A. Wong, Timeconvnets: A deep time windowed convolution neural network design for real-time video facial expression recognition, in: 2020 17th Conference on Computer and Robot Vision (CRV), 2020, pp. 9–16. doi:[10.1109/CRV50864.2020.00010](https://doi.org/10.1109/CRV50864.2020.00010).

[64] A. Bulat, J. M. Perez Rua, S. Sudhakaran, B. Martinez, G. Tzimiropoulos, Space-time mixing attention for video transformer, in: M. Ranzato, A. Beygelzimer, Y. Dauphin, P. Liang, J. W. Vaughan (Eds.), *Advances in Neural Information Processing Systems*, volume 34, Curran Associates, Inc., 2021, pp. 19594–19607. URL: <https://proceedings.neurips.cc/paper/2021/file/a34bacf839b923770b2c360eefa26748-Paper.pdf>.

[65] Z. Liu, J. Ning, Y. Cao, Y. Wei, Z. Zhang, S. Lin, H. Hu, Video swin transformer, in: *Proceedings of the IEEE/CVF Conference on Computer Vision and Pattern Recognition (CVPR)*, 2022, pp. 3202–3211.

[66] C. Szegedy, W. Liu, Y. Jia, P. Sermanet, S. Reed, D. Anguelov, D. Erhan, V. Vanhoucke, A. Rabinovich, Going deeper with convolutions, in: 2015 IEEE Conference on Computer Vision and Pattern Recognition (CVPR), 2015, pp. 1–9. doi:[10.1109/CVPR.2015.7298594](https://doi.org/10.1109/CVPR.2015.7298594).

[67] F. Zhang, Z. Li, B. Zhang, H. Du, B. Wang, X. Zhang, Multi-modal deep learning model for auxiliary diagnosis of alzheimer's disease, *Neurocomputing* 361 (2019) 185–195.

[68] G. Lee, K. Nho, B. Kang, K.-A. Sohn, D. Kim, Predicting alzheimer's disease progression using multi-modal deep learning approach, *Scientific reports* 9 (2019) 1952.

[69] F. Zhang, Z. Li, B. Zhang, H. Du, B. Wang, X. Zhang, Multi-modal deep learning model for auxiliary diagnosis of alzheimer's disease, *Neurocomputing* 361 (2019) 185–195.

[70] M. Liu, F. Li, H. Yan, K. Wang, Y. Ma, L. Shen, M. Xu, A multi-model deep convolutional neural network for automatic hippocampus segmentation and classification in alzheimer's disease, *NeuroImage* 208 (2020) 116459.

[71] W. Kang, L. Lin, B. Zhang, X. Shen, S. Wu, Multi-model and multi-slice ensemble learning architecture based on 2d convolutional neural networks for alzheimer's disease diagnosis, *Computers in Biology and Medicine* 136 (2021) 104678.

[72] S. Naz, A. Ashraf, A. Zaib, Transfer learning using freeze features for alzheimer neurological disorder detection using adni dataset, *Multimedia Systems* 28 (2022) 85–94.

[73] J. Sun, A. P. Fard, M. H. Mahoor, Xnodr and xnindr: Two accurate and fast fully connected layers for convolutional neural networks, *arXiv preprint arXiv:2111.10854* (2021).

[74] G. He, W. Zhao, X. Xia, R. Peng, X. Wu, An ensemble of shapelet-based classifiers on inter-class and intra-class imbalanced multivariate time series at the early stage, *Soft Computing* 23 (2019) 6097–6114.

[75] V. Sampath, I. Maurtua, J. J. Aguilar Martín, A. Gutierrez, A survey on generative adversarial networks for imbalance problems in computer vision tasks, *Journal of big Data* 8 (2021) 1–59.

[76] Z. Liu, P. Wei, Z. Wei, B. Yu, J. Jiang, W. Cao, J. Bian, Y. Chang, Towards Inter-class and Intra-class Imbalance in Class-imbalanced Learning, *arXiv e-prints* (2021) arXiv:2111.12791.

[77] A. H. Farzaneh, X. Qi, Discriminant distribution-agnostic loss for facial expression recognition in the wild, in: 2020 IEEE/CVF Conference on Computer Vision and Pattern Recognition Workshops (CVPRW), 2020, pp. 1631–1639. doi:[10.1109/CVPRW50498.2020.00211](https://doi.org/10.1109/CVPRW50498.2020.00211).

[78] Q. T. Ngo, S. Yoon, Weighted-center loss for facial expressions recognition, in: 2020 International Conference on Information and Communication Technology Convergence (ICTC), 2020, pp. 54–56. doi:[10.1109/ICTC49870.2020.9289472](https://doi.org/10.1109/ICTC49870.2020.9289472).

[79] A. H. Farzaneh, X. Qi, Facial expression recognition in the wild via deep attentive center loss, in: *Proceedings of the IEEE/CVF Winter Conference on Applications of Computer Vision (WACV)*, 2021, pp. 2402–2411.

[80] Y. Tian, M. Li, D. Wang, Dfer-net: Recognizing facial expression in the wild, in: 2021 IEEE International Conference on Image Processing (ICIP), 2021, pp. 2334–2338. doi:[10.1109/ICIP42928.2021.9506770](https://doi.org/10.1109/ICIP42928.2021.9506770).

[81] J. Deng, J. Guo, E. Ververas, I. Kotsia, S. Zafeiriou, Retinaface: Single-shot multi-level face localisation in the wild, in: *Proceedings of the IEEE/CVF conference on computer vision and pattern recognition*, 2020, pp. 5203–5212.

[82] L. A. McNamara, S. W. Martin, 1 - principles of epidemiology and public health, in: S. S. Long (Ed.), *Principles and Practice of Pediatric Infectious Diseases* (Sixth Edition), sixth edition ed., Elsevier, Philadelphia, 2023, pp. 1–9.e1. URL: <https://www.sciencedirect.com/science/article/pii/B978032375608200001X>. doi:<https://doi.org/10.1016/B978-0-323-75608-2.00001-X>.